Surface mass-balance changes of the Greenland ice sheet since 1866

L.M. WAKE,[1] P. HUYBRECHTS,[2,3] J.E. BOX,[4,5] E. HANNA,[6] I. JANSSENS,[2] G.A. MILNE[1]

[1]*Department of Earth Sciences, Durham University, Science Laboratories, South Road, Durham DH1 3LE, UK*
E-mail: l.m.wake@durham.ac.uk
[2]*Departement Geografie, Vrije Universiteit Brussel, Pleinlaan 2, B-1050 Brussels, Belgium*
[3]*Alfred-Wegener-Institut für Polar- und Meeresforschung, Postfach 120161, D-27515 Bremerhaven, Germany*
[4]*Byrd Polar Research Center, The Ohio State University, 1090 Carmack Road, Columbus, OH 43210-1002, USA*
[5]*Atmospheric Sciences Program, Department of Geography, The Ohio State University, Columbus, OH 434210-136, USA*
[6]*Department of Geography, University of Sheffield, Sheffield S10 2TN, UK*

ABSTRACT. Mass loss from the Greenland ice sheet over the past decade has caused the impression that the ice sheet has been behaving anomalously to the warming of the 1990s. We have reconstructed the recent (1866–2005) surface mass-balance (SMB) history of the Greenland ice sheet on a 5×5 km grid using a runoff-retention model based on the positive degree-day method. The model is forced with new datasets of temperature and precipitation patterns dating back to 1866. We use an innovative method to account for the influence of year-on-year surface elevation changes on SMB estimates and have found this effect to be minor. All SMB estimates are made relative to the 1961–90 average SMB and we compare annual SMB estimates from the period 1995–2005 to a similar period in the past (1923–33) where SMB was comparable, and conclude that the present-day changes are not exceptional within the last 140 years. Peripheral thinning has dominated the SMB response during the past decade, as in 1923–33, but we also show that thinning was not restricted to the margins during this earlier period.

INTRODUCTION

Owing to their potential impact on ocean–atmosphere circulation and global sea-level change, the stability of the Earth's large ice sheets is central to the topic of global change in response to a projected climate warming. The recent Intergovernmental Panel on Climate Change (IPCC) report (Lemke and others, 2007) summarizes various efforts in estimating the mass balance of the Greenland ice sheet. These estimates are in disagreement but they do highlight an increasing rate of mass loss from Greenland during the past 5–10 years.

Recent geodetic observations have shed light on the patterns and magnitude of surface elevation change. Combining the results of laser altimeter surveys and snowfall/melt modelling, Krabill and others (2004) demonstrated that average ice loss between 1993 and 1998 was 60 km^3 a^{-1} ice equivalent (55 Gt a^{-1}) and between 1997 and 2003 was 80 ± 12 km^3 a^{-1} ice equivalent (73 Gt a^{-1}) (all volume changes are henceforward quoted in ice equivalent). According to a separate study (Zwally and others, 2005), the Greenland ice sheet produced a small overall gain of 12 ± 3.3 Gt a^{-1} during 1992–2002. Variation in estimates of mass loss from altimeter studies is the likely result of the particular treatment adopted to account for snow compaction and densification. With the onset of the Gravity Recovery and Climate Experiment (GRACE) in 2002, the bigger picture of mass loss from Greenland has been revealed. After corrections for land hydrology and glacial isostatic adjustment-related (GIA-related) mass changes, Greenland is showing an overall decline in mass balance from 2002 to 2006. The most recent estimates from the GRACE satellite over 2003–05 indicate a mass loss of 101 ± 16 Gt a^{-1} (110 km^3 a^{-1}) with accumulation at elevations higher than 2000 m and loss below 2000 m

(Luthcke and others, 2006). An overlapping period of data (2002–06) was analysed in a later study where a loss of 248 ± 36 km^3 a^{-1} was detected (Velicogna and Wahr, 2006). Although there is disagreement in the absolute values of mass loss, it is clear that: (1) the ice sheet is in a negative balance; and (2) the rate of mass loss has been increasing over the last decade.

The primary mechanisms of mass loss are the discharge of ice into the ocean via outlet glaciers (see Fig. 1) and runoff of surface melt. Annual variations in outlet glacier discharge have been recorded in glaciers in southeast Greenland (Rignot and others, 2004; Howat and others, 2005, 2007), indicating that these systems may be capable of responding to annual climatic changes. Greenland's largest outlet glacier, Jakobshavn Isbræ, has been studied since 1992, with velocity variations apparently coinciding with periods of thickening and thinning (Joughin and others, 2004). The Jakobshavn terminus retreated over the past 30 years (Sohn and others, 1998), with calving rate mirroring variations in glacier speed (Joughin and others, 2004). Rignot and Kanagaratnam (2006) estimate a discharge of 23.6 km^3 a^{-1} from Jakobshavn during 1996–2000. Conversely, the doubling of glacier velocity recorded over the period 1985–2003 by Joughin and others (2004) is interpreted to produce an increase in glacier discharge from 26.5 km^3 a^{-1} (1985) to 50 km^3 a^{-1} (2003). Other major contributions to mass loss during 1996–2000 arise from glaciers in the east (Rignot and Kanagaratnam, 2006): Kangerdlugssuaq (27.8 km^3 a^{-1}) and Helheim (26.3 km^3 a^{-1}), as well as a total discharge of 67 km^3 a^{-1} from a collection of smaller glaciers in southeast Greenland. A recent study by Howat and others (2007) on some east coast outlet glaciers has shown a doubling in mass loss in under a year (2004), but their combined rate of mass loss had decreased in 2006. The response of Greenland's surface mass balance

Fig. 1. Map of locations and features mentioned in the text: towns (red), regions (black) and outlet glaciers (blue).

Fig. 2. (a) Mean annual temperature (TMA) difference averaged over ice-sheet area, assembled from two datasets: ECMWF re-analyses (blue) and BOX (red). (b) Annual precipitation ratio averaged over ice-sheet area. Colour convention as in (a).

to climatic changes over the last 150 years is not as well studied and is investigated in this study. Previously published model estimates based on the positive degree-day method (Janssens and Huybrechts, 2000) show a decrease in surface mass balance between 1993 and 1998 ($-15 \pm 60 \, \mathrm{km^3 \, a^{-1}}$) and between 1998 and 2003 ($-40 \pm 65 \, \mathrm{km^3 \, a^{-1}}$) (Hanna and others, 2005), but error bars on the estimates indicate that the overall sign of the mass balance may be either positive or negative. Box and others (2006b) suggest an ice mass loss of about $100 \, \mathrm{km^3 \, a^{-1}}$ for the period 1988–2004, after a correction for glacier discharge and subglacial melting.

In this paper, we present a time series of the annual surface mass balance (SMB) of the Greenland ice sheet for the period 1866–2005. Values of SMB are quoted with respect to the average value for the 1961–90 climatological normal period. In addition, we report on how the spatial patterns of SMB vary over specified historic time intervals. This will place into context the current behaviour of the ice sheet, and specifically how SMB has varied both spatially and temporally during the late 19th century and early 21st century. Patterns of SMB are important indicators of the stability of an ice sheet under the present meteorological conditions. For example, peripheral thinning of an ice sheet and migration of the equilibrium line towards higher elevations denote that the ice sheet may be in a positive feedback cycle of decay. These observations provide more insight than measurements of outlet glacier discharge made over only a few years, which are shown to have interannual fluctuation (Howat and others, 2007). A brief discussion of the mass-balance model is given, in which we briefly assess the impact of excluding elevation changes in SMB calculations. We then discuss the results and focus, in particular, on two applications: (1) comparison of the response of the ice sheet to a recent period of warming and
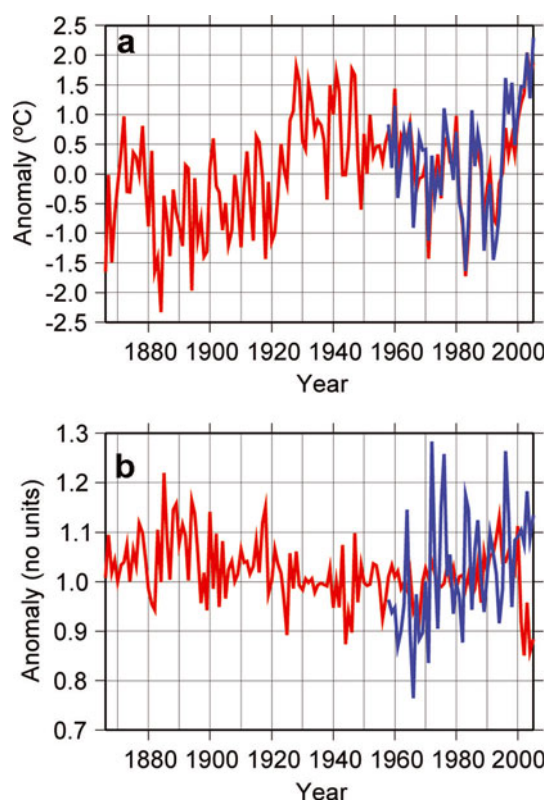
a similar warm period during the 1920s (Chylek and others, 2006) to examine how exceptional the recent changes are within a longer time context; and (2) comparison of the model to observations of surface elevation changes from 1995 to 2005 to gauge qualitatively the relative contribution of SMB changes in the observed total surface changes.

DATA AND TECHNIQUES

Mass balance was calculated by applying a runoff-retention model (Janssens and Huybrechts, 2000) based on the positive degree-day (PDD) method (Braithwaite and Olesen, 1989; Reeh, 1991). The model is forced using monthly temperature and annual precipitation minus evaporation ($P - E$) datasets from two sources. From 1866 to 1957, we input climatic data assembled from a spatio-temporal correlation between coastal meteorological and ice-core data and Polar MM5 output (Box and others, 2006a, 2008), hereafter named 'BOX'. From 1958 to 2005, we use data assembled from European Centre for Medium-Range Weather Forecasts F-ERA40 reanalyses (Hanna and others, 2008), named 'ECMWF'. These data, shown in Figure 2, are projected onto a $5 \times 5 \, \mathrm{km}$ grid, on which the SMB is calculated at monthly intervals and integrated over the entire ice sheet to give an overall annual mass-balance figure.

This study extends the work of Hanna and others (2005, 2008) in two important respects. The period considered is longer (1866–2005 compared with 1958–2003) and we apply climate forcing in 'anomaly mode' to reduce sensitivity to biases in the input time series of precipitation

and temperature. The temperature and precipitation are reduced to anomalies with respect to a baseline average established using the climate datasets. The parameterized temperature and precipitation fields are perturbed by their respective anomalies (see later in this section). A critical step required to run the model in anomaly mode is the selection of a baseline period during which the climatic variation is representative of a longer-term average. The length of the baseline period must be sufficiently long such that the occurrence of rare and extreme climate events does not significantly influence estimates of longer-term averages. We choose 1961–90 as our baseline period. Hanna and others (2005) found this period to be very close to a balanced total mass budget averaged over the entire ice sheet. For our analysis we make the working assumption that such a balance is also valid down to the level of individual drainage basins, although it is not possible to support this assertion with strong evidence. Also, our reference precipitation dataset is homogenized to the 1961–90 climate and is therefore representative of this period (Huybrechts and others, 2004).

For each point (x, longitude; y, latitude) on the ice sheet, we reduce the original datasets to their monthly (t_m) or annual (t_a) anomalies by the following methods:

$$T_{anom}(x, y, t_m) = T(x, y, t_m) - \bar{T}(x, y, 1961-90_m) \quad (1)$$

$$P_{anom}(x, y, t_a) = P(x, y, t_a)/\bar{P}(x, y, 1961-90_a). \quad (2)$$

It was necessary to splice the two datasets because the ECMWF datasets only extend back to 1958, and their use is favoured after 1958 because the data are reasonably well validated (Hanna and Valdes, 2001; Hanna and others, 2001). We use the BOX dataset to extend back to 1866. Also, by applying the model in anomaly mode, any trend or bias introduced by splicing the two different climate time series is removed. Figure 2a shows the overlap achieved by splicing the two temperature datasets. From 1958 onwards, both datasets mirror each other well and we can therefore be confident that switching to the second dataset will not distort our results pre-1958. Over the climatological normal period 1961–90, neither dataset shows a convincing increase/decrease of mean annual temperature (TMA), but both show comparable trends (BOX: $-0.02 \pm 0.69°C \, a^{-1}$; ECMWF: $-0.02 \pm 0.77°C \, a^{-1}$). The striking feature of the temperature series is the longer period (50 years) variation imprinted on the annual variation. Significant increases in temperature anomaly are recorded about 1920 and 1995. We observe that the appearances of the precipitation anomaly series provided by the two datasets are very different (Fig. 2b). The BOX dataset shows lower variation and no discernible trend over our selected baseline period ($-0.0001 \pm 0.0008 \, a^{-1}$). We calculate an increase of $0.005 \pm 0.0025 \, a^{-1}$ in the ECMWF data, which is different in sign and 50 times that recorded in the BOX dataset. The reason for the difference between the datasets is not known, but since no significant trend in our baseline period is recorded in either dataset, there is little consequence in the fact that the variability is not consistent.

The monthly temperature at each point on the grid is a sum of the parameterized temperature (Huybrechts and de Wolde, 1999) plus the anomaly (T_{anom}). The parameterized temperature depends on elevation and latitude and follows a cosine function over the year. Mean annual temperature (TMA, in °C) is described by a linear function and is dependent on latitude and elevation (in metres) as adapted from Reeh (1991):

$$TMA(x, y) = 49.19 - [0.007992 \times elevation - (0.7576y)] \quad (3)$$

The near-surface temperature inversion is accounted for at higher latitudes by the following equation:

$$Threshold = 20(y - 65). \quad (4)$$

If the elevation is below the threshold value for a particular location, then the elevation term in the parameterization for TMA is substituted with the threshold value calculated above. Mean July temperature (TMJ) also follows a linear function, for $t_m = 7$, i.e. the seventh month:

$$TMJ(x, y, 7) = 30.78 - (0.006277 \times elevation) - (0.3262y). \quad (5)$$

Monthly temperatures (T) are calculated (for $t_m = 1, 12$):

$$T(x, y, t_m) = TMA - |(TMA - TMJ)| \cdot cos[(\pi/6)(t_m - 1)] + T_{anom}(x, y, t_m). \quad (6)$$

The positive degree-days (PDDs, units: °C-day) are calculated using the scheme applied in Janssens and Huybrechts (2000) and take into account monthly deviations of the temperature from the monthly average. We treat the precipitation series differently. A precipitation field known to be representative of the 1961–90 average (Huybrechts and others, 2004) is perturbed on an annual basis by the fractional difference in precipitation for the year compared with the 1961–90 annual average (P_{anom}). This produces a predicted annual precipitation for each point on the surface. Whether this precipitation falls as rain or snow depends on the amount of time the surface temperature remains above or below a predefined temperature threshold of 1°C, respectively. Rain is immediately added to the liquid-water (melt) term. Snow is melted first at a rate of 2.7 mm w.e. °C^{-1} d^{-1}, also liberating any capillary water that may be trapped. This melt then has the possibility to be retained and is proportional to the original snow cover and surface temperature. It will then be retained as superimposed ice. Any unfrozen water remaining is added to capillary water until saturation of the snow cover. After saturation, residual water is runoff (Pfeffer and others, 1991). Once all snow has disappeared, any remaining PDDs are used to melt superimposed ice, if any, and then glacier ice, which melts at a higher rate of 7.2 mm w.e. °C^{-1} d^{-1}. The water gained from this stage is added to the runoff. We apply the retention model 'pr_capil' described in Janssens and Huybrechts (2000). This takes into account refreezing and capillary water retention within the snowpack. We refer the reader to Janssens and Huybrechts (2000) for further insight. SMB is defined as rain and snow minus runoff. We note that degree-day factors are highly variable around Greenland, and that calculated runoff is highly sensitive to these values. The values quoted here are fixed spatially and temporally and are almost the same as those used in Braithwaite and Olesen (1989), and are within the range of values reported by Braithwaite (1995). We use an innovative technique to investigate the influence of annual surface elevation changes on SMB prediction, and to correct the adopted elevation dataset (valid for 1994; Bamber and others, 2001). This will facilitate the realistic representation of elevation-related temperature, and therefore SMB. We treat the change of ice-sheet elevation due to changes in
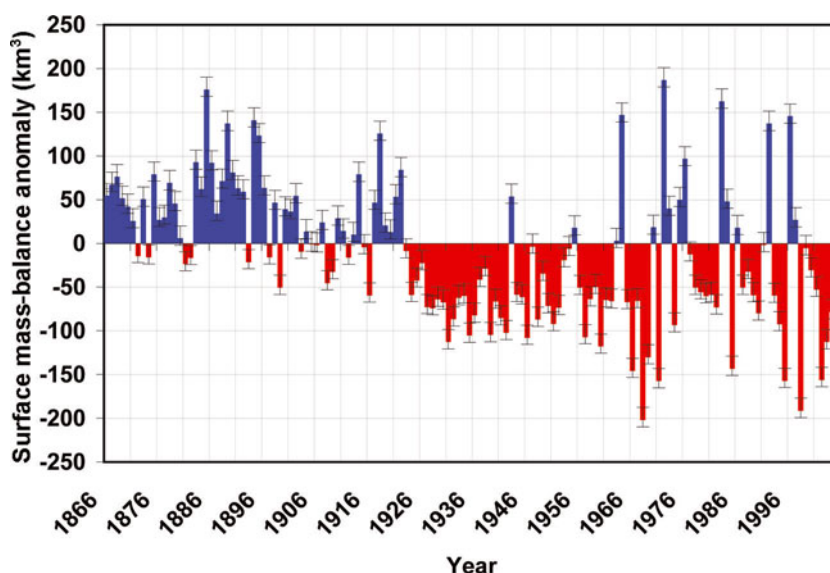
Fig. 3. Time series of annual surface mass-balance anomalies for the period 1866–2005. Values are quoted in km^3 ice equivalent.

SMB (in ice equivalent and ignoring changes in density profiles) as follows:

$$\partial H(x, y, t) = \mathrm{SMB}(x, y, t) - \overline{\mathrm{SMB}(x, y, 1961{-}90)} \quad (7)$$

where ∂H is the local surface elevation change arising from an SMB change in 1 year for a point on the ice sheet and SMB is the local SMB defined on an annual basis either at time 't' or as the average for the period 1961–90. For equilibrium at a point on the ice sheet (assumed for the period 1961–90), $\partial H = 0$. Any deviation from zero will result in a change of elevation.

There are a number of assumptions implicit in the method described above. For example: (1) the parameterized monthly temperatures are valid for the 1961–90 period (i.e. in the first approximation, the 1994 elevation produces temperatures representative of the 1961–90 monthly means); (2) the ice-sheet surface is in equilibrium with the 1961–90 average climate; and (3) from (2) we implicitly assume that the 1961–90 ice flow is constant over the whole integration period considered here. To correct for the effect of surface elevation changes on surface temperature, and hence SMB, we sum the elevation changes from the start of the model run (1866) until 1994 and correct the original elevation by this amount, and re-run the model until satisfactory convergence of ice-sheet averaged SMB with the original SMB calculated from the 1994 elevation dataset. By doing this, we can be confident that we are using a fairly realistic representation of the 1866 surface elevation. The model arrives at a similar prediction for 1994 SMB after two iterations. We assume $\partial H(x, y, t)$ equates directly to a change in surface elevation and correct the original surface elevation grid at each point in the same way.

Surface mass-balance results are biased if we use uncorrected elevation grids to predict parameterized temperature. From 1866 to 1994 we model a small rate of mass loss of 0.77 km^3 a^{-1}. The consequence for the surface elevation is that when using the uncorrected dataset the surface elevation for the start of the time series (1866) is lower than it should be and we will predict a less positive SMB. If these effects are ignored, our analysis found that the predicted SMB is altered by on average 2 km^3 a^{-1}. If, during the period 1866–1994, the average SMB was highly positive or negative, correcting the reference elevation dataset would be essential.

RESULTS AND DISCUSSION

Figure 3 shows the calculated changes in SMB with respect to the 1961–90 average. Analysis of the SMB time series shows that the ice sheet was slightly losing surface mass overall during the period 1961–90. Even though the input climate data suggest that there is no trend in the climate anomalies over this period, the ice sheet is still responding to year-on-year non-zero perturbations in temperature and precipitation. The anomalies in temperature and precipitation do not balance each other to give an exactly zero SMB anomaly. The model indicates that the ice sheet is in an overall state of mass loss, and this neither accelerates nor decelerates significantly over the baseline period (+0.62 ± 2 km^3 a^{-1}). We were unable to replicate such a close state of dynamic equilibrium with the use of other climatological normal baselines (e.g. 1971–2000).

There are a number of features evident in Figure 3. For the first 60 years of the study period, the ice sheet was mainly in a state of positive SMB with respect to 1961–90. This reflects the fact that temperatures in this period are lower than the 1961–90 average in Greenland and worldwide. There is a distinct change to a period of prolonged negative SMB anomalies at about 1925 that persisted until about 1960. This change is clearly related to the relatively high temperatures experienced during this period, particularly between the mid-1920s and 1950. Between 1970 and the end of the 20th century the SMB predictions display high variability but give, on average, a slightly negative SMB anomaly. The final 6 years of the study period indicate a distinct and consistent negative mass-balance anomaly which correlates well with the elevated temperatures shown in Figure 2. Over the entire period (1866–2005), the overall SMB of the ice sheet is almost constant, with surface volume being lost at a rate of 0.89 ± 0.15 km^3 a^{-1} based on a straightforward linear regression of the SMB time series. Figure 4 shows the spatial pattern of the cumulated SMB for
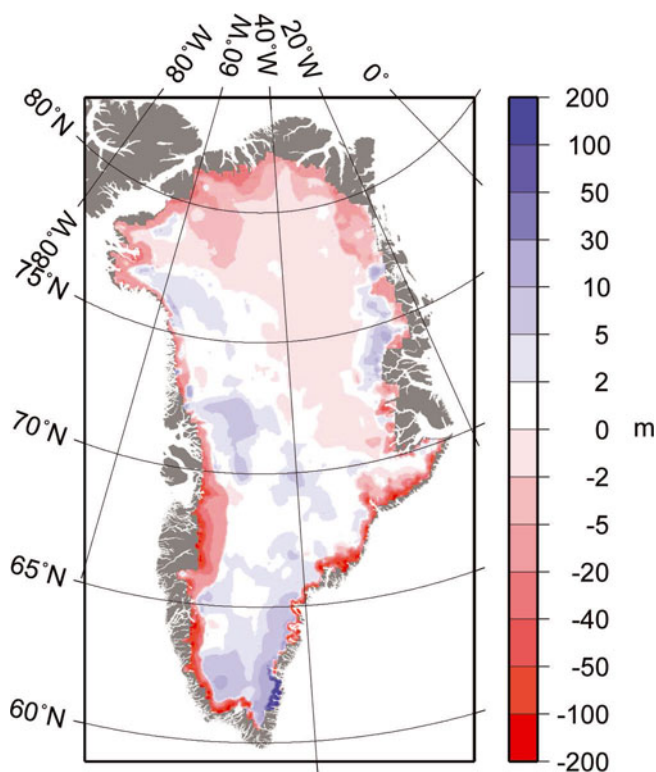
Fig. 4. Spatial pattern of total cumulated surface mass-balance change for the period 1866–2005. Values are in metres ice equivalent.

the entire study period and indicates that most of the ice has been lost at the margin, with some areas having lost over 150 m of ice since 1866. A feature persistent in time is the sharp transition between positive and negative cumulated SMB anomaly along the ice margin in the south and east. Although southeast Greenland receives high amounts of accumulation, the topography of East Greenland is steep, so the ablation zone is narrow compared with the west of Greenland. In the central portion of the ice sheet, a northeast/southwest divide of net lowering and net growth (respectively) is visible. Overall, the maximum amount of surface ice lost in this area is 5 m, with a maximum of 5–10 m gained over some areas in the southwest.

The time series presented in Figure 3 provides a unique record of the mass-balance response of the Greenland ice sheet to temperature and precipitation variations during the past 140 years. Since much current attention is focused on the response of the Greenland ice sheet to the temperature increase over the past decade, an interesting application of our results is to place the more recent changes within a longer time context. A noticeable feature of the time series (Fig. 3) is the transition from lengthy periods of positive (1866–1922) to negative (1923–53) SMB anomalies. This first sequence of positive SMB anomalies corresponds to the Greenland ice sheet emerging from the Little Ice Age. The Little Ice Age is a prolonged period of cooling beginning after the 'Medieval Warm Epoch' (approximately AD 1200) and lasting until the early 20th century. During this period (1866–1922) we model an average annual SMB anomaly of $37 \pm 11 \, \mathrm{km^3 \, a^{-1}}$. Csatho and others (2008) detected a period of thinning of Jakobshavn Isbræ during 1902–13, and linked this behaviour to the interaction of the ice dynamics with changes upstream of Jakobshavn Isbræ. We model an

average annual ice loss of approximately $5 \, \mathrm{m \, a^{-1}}$ between 65° N and 70° N on the western margins of the ice sheet, even though the majority of the ice sheet is in a state of positive mass balance. Interestingly, our results also show an area of thinning (average ice loss 0.02–0.10 m a⁻¹) during 1902–13 in the drainage area east of Jakobshavn Isbræ between 68.5°N and 69.0°N and extending up to 500 km inland in an east-southeast direction (not shown here). After this, the Greenland ice sheet displays 40 years of high-amplitude variation. We have identified two periods when the average annual SMB was similar to the 1961–90 average (1995–2005: $-69 \, \mathrm{km^3 \, a^{-1}}$; 1923–33: $-67 \, \mathrm{km^3 \, a^{-1}}$). During 1995–2005, the rate of increase of TMA was almost twice that of the earlier period, and there are no discernible trends in the precipitation anomalies of either period (1995–2005: $-0.007 \pm 0.008 \, \mathrm{a^{-1}}$; 1923–33: $0.003 \pm 0.004 \, \mathrm{a^{-1}}$). The rate of change of mean summer temperature (June, July and August) averaged over the ice-sheet area for the two periods is $0.17°\mathrm{C \, a^{-1}}$ (1995–2005) and $0.04°\mathrm{C \, a^{-1}}$ (1923–33), respectively. In effect, we are seeing the same overall SMB response during 1923–33, but under a smaller increase in rate of change of mean annual and summer temperature than that experienced during 1995–2005.

The spatial patterns of the SMB changes during these two periods are not similar (Fig. 5). Both show high rates of peripheral lowering, but a larger area of the ice sheet displayed negative SMB anomalies during 1923–33. Much of this thinning during 1923–33 appears to have occurred in the accumulation area, with this lowering being driven by lower than average accumulation rates rather than higher than average ablation rates. The extensive growth for 1995–2005 was not sufficient to counteract the high (5–10 m a⁻¹) rates of peripheral lowering. The growth–thinning transition in the southeast is absent from the earlier period, but is a significant feature during 1995–2005. During the period 1923–33, the average TMA anomaly over the ice sheet increased by 0.75°C compared with 1.9°C for 1995–2005. The Greenland ice sheet overall has therefore responded in a similar fashion to a smaller temperature increase in the early 20th century, indicating that the current changes are not entirely exceptional. Neither time period exhibits a pattern of loss that is comparable to the long-term net SMB change (Fig. 4). Based on the simulations of these two periods, it could as well be stated that the recent changes that have been monitored extensively (Krabill and others, 2004; Luthcke and others, 2006; Thomas and others, 2006) are representative of natural sub-decadal fluctuations in the mass balance of the ice sheet and are not necessarily the result of anthropogenic-related warming.

Our predictions of ice loss due to SMB compare favourably to published studies of surface elevation changes. For 1997–2003, we model an average ice loss of $-82 \, \mathrm{km^3 \, a^{-1}}$, comparable to values obtained by Krabill and others (2004). Laser altimeter studies by Thomas and others (2006) record a doubling in mass loss over two periods 1993–98 and 1998–2004 (4–$50 \, \mathrm{Gt \, a^{-1}}$ and 57–$105 \, \mathrm{Gt \, a^{-1}}$). We predict a similar pattern for the two periods ($-59 \, \mathrm{Gt \, a^{-1}}$ and $-97 \, \mathrm{Gt \, a^{-1}}$, respectively). By matching our results with Krabill and others (2004) and Thomas and others (2006), it may be interpreted that many of the observed trends are caused mainly by changes in SMB. However, we are not able to make firm conclusions on the respective role of ice dynamics vs SMB changes on elevation changes because our assumption of equilibrium for 1961–90 may not hold for individual points
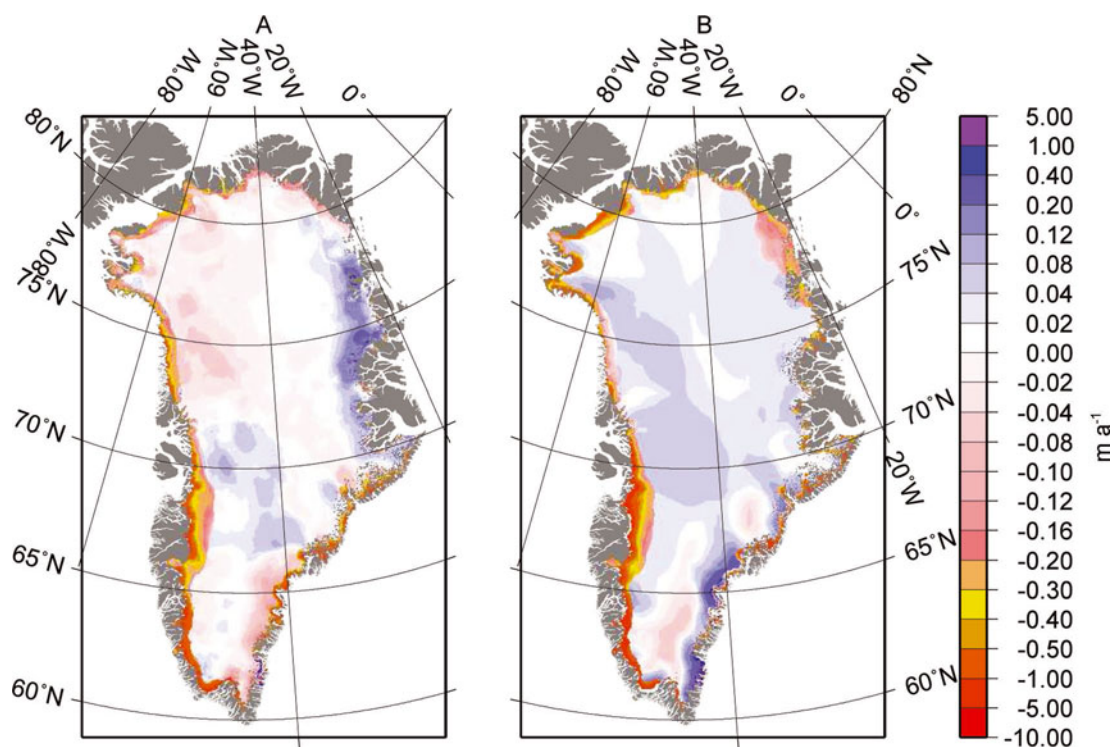
Fig. 5. Rate of change of surface mass-balance anomaly (calculated by linear regression) for the periods (a) 1923–33 and (b) 1995–2005. Values are in metres per year ice equivalent.

on our grid, even if such a balance has stronger support for the Greenland ice sheet as a whole.

Comparison of recent laser altimetry (2000) and older digital elevation models (1985) made by Podlech and others (2004) shows that during 1985–2005 the area around Sermilik Glacier in South Greenland (Fig. 1) lost 90 m of ice at approximately the 500 m elevation contour. In this area, we model losses in the range 100–200 m. These are larger than the values obtained from observations, but lie in the range (–90 to –130 m) calculated by Podlech and others (2004). For the higher-elevation bands (500–750 m and 750–1000 m) our predictions differ with the measurements; we still model a significant annual average thinning of 8–12 $m\,a^{-1}$. Again, this is likely to be a consequence of our assumption of ice-sheet-wide equilibrium for 1961–90.

Over the measurement period 1997–2003, our modelling of SMB reflects some features of Krabill and others (2004) such as (our data not pictured): lowering in the area of Kong Frederik VIII Land in the north (77–80° N, 20–30° W) and near balance in the central area north of 73° N. However, there are also some important differences: the work of Krabill and others (2004) reveals a wider area of negative elevation change in the eastern half of Greenland, whereas we model only localized (up to 20 km) wide areas of extreme (>5–10 $m\,a^{-1}$) surface lowering. Over the same period, we model considerable (0.3–1.0 $m\,a^{-1}$) thinning on the south dome of the Greenland ice sheet, where Krabill and others (2004) measure thickening of about 0.1 $m\,a^{-1}$. Omission of finer-scale details that are present in our study is the likely result of interpolation between flight-lines. Our patterns of change bear more similarity to those of Thomas and others (2006) for the period 1993–98. We see a similar pattern of near balance to slight (0.1 $m\,a^{-1}$) thickening through much of the central portions of the ice sheet. Although the resolution of Thomas and others' study is ten times less than ours, it picks out important small-scale features present in our study: thinning of >0.6 $m\,a^{-1}$ between 65° N and 70° N east of Jakobshavn, and extreme thinning in Kong Frederik VIII Land (see Fig. 1) and in a narrow (<20 km) band between Savissivik (76.023° N, 65.081° W) and Upernavik (72.78° N, 56.17° W) in the northwest.

CONCLUSION

We have presented a modelling study tracking SMB changes of the Greenland ice sheet since 1866, reflecting how the ice sheet has behaved under the climatic conditions of the 19th–21st centuries. Over the time window of our study, we find that the Greenland ice sheet has reacted to, and endured, a temperature increase similar to that experienced at present. Higher surface runoff rates similar to those of the last decade were also present in an earlier warm period in the 1920s and 1930s and apparently did not lead to a strong feedback cycle through surface lowering and increased ice discharge. Judging by the volume loss in these periods, we can interpret that the current climate of Greenland is not causing any exceptional changes in the ice sheet. Mass loss through glacier discharge is currently believed to dominate mass loss through SMB, and both processes are likely to be correlated. Forman and others (2007) report that the ice sheet retreated 1–2 km inland at Kangerlussuaq, West Greenland, over the past 100 years. Although our model resolution is 5 × 5 km, we predict complete disappearance of some ice-sheet points in this area, in line with these observations. We are not able to shed light on the relative contributions of ice dynamics vs SMB to the current mass loss, but our study puts the modern-day changes into the context of longer-term century time-scale changes.

REFERENCES

Bamber, J.L., S. Ekholm and W.B. Krabill. 2001. A new, high-resolution digital elevation model of Greenland fully validated with airborne laser altimeter data. *J. Geophys. Res.,* **106**(B4), 6733–6745.

Box, J.E., D.H. Bromwich and E. Mosley-Thompson. 2006a. A centry-plus perspective on Greenland ice sheet mass balance. *Eos.,* **87**(52), Fall Meet. Suppl., Abstract U22A-03

Box, J.E. *and 8 others.* 2006b. Greenland ice sheet surface mass balance variability (1988–2004) from calibrated polar MM5 output. *J. Climate,* **19**(12), 2783–2800.

Box, J.E., L. Yang, D.H. Bromwich and L. Bai. 2008. Greenland ice sheet surface air temperature and accumulation rate reconstruction (1840–2007) from in-situ data records. *Eos.,* **89**(53), Fall Meet. Suppl., Abstract U22A-03

Braithwaite, R.J. 1995. Positive degree-day factors for ablation on the Greenland ice sheet studied by energy-balance modelling. *J. Glaciol.,* **41**(137), 153–160.

Braithwaite, R.J. and O.B. Olesen. 1989. Calculation of glacier ablation from air temperature, West Greenland. *In* Oerlemans, J., *ed. Glacier fluctuations and climatic change.* Dordrecht, Kluwer Academic Publishers, 219–233.

Chylek, P., M.K. Dubey and G. Lesins. 2006. Greenland warming of 1920–1930 and 1995–2005. *Geophys. Res. Lett.,* **33**(11), L11707. (10.1029/2006GL026510.)

Csatho, B., T. Schenk, C.J. van der Veen and W.B. Krabill. 2008. Intermittent thinning of Jakobshavn Isbræ, West Greenland, since the Little Ice Age. *J. Glaciol.,* **53**(184), 131–144.

Forman, S.L., L. Marín, C. van der Veen, C. Tremper and B. Csatho. 2007. Little Ice Age and neoglacial landforms at the Inland Ice margin, Isunguata Sermia, Kangerlussuaq, west Greenland. *Boreas,* **36**(4), 341–351.

Hanna, E. and P. Valdes. 2001. Validation of ECMWF (re)analysis surface climate data, 1979–1998, for Greenland and implications for mass balance modelling of the ice sheet. *Int. J. Climatol.,* **21**(2), 171–195.

Hanna, E., P. Valdes and J. McConnell. 2001. Patterns and variations of snow accumulation over Greenland, 1979–98, from ECMWF analyses and their verification. *J. Climate,* **14**(17), 3521–3535.

Hanna, E., P. Huybrechts, I. Janssens, J. Cappelen, K. Steffen and A. Stephens. 2005. Runoff and mass balance of the Greenland ice sheet: 1958–2003. *J. Geophys. Res.,* **110**(D13), D13108. (10.1029/2004JD005641.)

Hanna, E. *and 8 others.* 2008. Increased runoff from melt from the Greenland Ice Sheet: a response to global warming. *J. Climate,* **21**(2), 331–341.

Howat, I.M., I. Joughin, S. Tulaczyk and S. Gogineni. 2005. Rapid retreat and acceleration of Helheim Glacier, east Greenland. *Geophys. Res. Lett.,* **32**(22), L22502. (10.1029/2005GL024737.)

Howat, I.M., I.R. Joughin and T.A. Scambos. 2007. Rapid changes in ice discharge from Greenland outlet glaciers. *Science,* **315**(5818), 1559–1561.

Huybrechts, P. and J. de Wolde. 1999. The dynamic response of the Greenland and Antarctic ice sheets to multiple-century climatic warming. *J. Climate,* **12**(8), 2169–2188.

Huybrechts, P., J. Gregory, I. Janssens and M. Wild. 2004. Modelling Antarctic and Greenland volume changes during the 20th and 21st centuries forced by GCM time slice integrations. *Global Planet. Change,* **42**(1–4), 83–105.

Janssens, I. and P. Huybrechts. 2000. The treatment of meltwater retardation in mass-balance parameterizations of the Greenland ice sheet. *Ann. Glaciol.,* **31**, 133–140.

Joughin, I., W. Abdalati and M.A. Fahnestock. 2004. Large fluctuations in speed on Greenland's Jakobshavn Isbræ glacier. *Nature,* **432**(7017), 608–610.

Krabill, W. *and 12 others.* 2004. Greenland Ice Sheet: increased coastal thinning. *Geophys. Res. Lett.,* **31**(24), L24402. (10.1029/2004GL021533.)

Lemke, P. *and 10 others.* 2007. Observations: changes in snow, ice and frozen ground. *In* Solomon, S. *and 7 others, eds. Climate change 2007: the physical science basis. Contribution of Working Group I to the Fourth Assessment Report of the Intergovernmental Panel on Climate Change.* Cambridge, etc., Cambridge University Press, 337–383.

Luthcke, S.B. *and 8 others.* 2006. Recent Greenland ice mass loss by drainage system from satellite gravity observations. *Science,* **314**(5803), 1286–1289.

Pfeffer, W.T., M.F. Meier and T.H. Illangasekare. 1991. Retention of Greenland runoff by refreezing: implications for projected future sea level change. *J. Geophys. Res.,* **96**(C12), 22,117–22,124.

Podlech, S., C. Mayer and C.E. Bøggild. 2004. Glacier retreat, mass-balance and thinning: the Qagssimiut ice margin, South Greenland. *Geogr. Ann.,* **86A**(4), 305–317.

Reeh, N. 1991. Parameterization of melt rate and surface temperature on the Greenland ice sheet. *Polarforschung,* **59**(3), 113–128.

Rignot, E. and P. Kanagaratnam. 2006. Changes in the velocity structure of the Greenland Ice Sheet. *Science,* **311**(5673), 986–990.

Rignot, E., D. Braaten, P. Gogineni, W.B. Krabill and J.R. McConnell. 2004. Rapid ice discharge from southeast Greenland glaciers. *Geophys. Res. Lett.,* **31**(10), L10401. (10.1029/2004GL019474.)

Sohn, H.G., K.C. Jezek and C.J. van der Veen. 1998. Jakobshavn Glacier, West Greenland: 30 years of spaceborne observations. *Geophys. Res. Lett.,* **25**(14), 2699–2702.

Thomas, R., E. Frederick, W. Krabill, S. Manizade and C. Martin. 2006. Progressive increase in ice loss from Greenland. *Geophys. Res. Lett.,* **33**(10), L10503. (10.1029/2006GL026075.)

Velicogna, I. and J. Wahr. 2006. Acceleration of Greenland ice mass loss in spring 2004. *Nature,* **443**(7109), 329–331.

Zwally, H.J. *and 7 others.* 2005. Mass changes of the Greenland and Antarctic ice sheets and shelves and contributions to sea-level rise: 1992–2002. *J. Glaciol.,* **51**(175), 509–527.